Forsch Ingenieurwes (2019) 83:751–757
https://doi.org/10.1007/s10010-019-00353-6

ORIGINALARBEITEN/ORIGINALS

A new worm grinding method of face gears based on the optimization of dressing wheel profile

Xianlin Shi[1,2] · Yuansheng Zhou[1,2] · Wuji Zhang[1,2] · Jinyuan Tang[1,2]

Received: 30 March 2019 / Accepted: 26 June 2019

Abstract

Face gear drives have been well applied in high-speed and heavy load applications. Due to the strict requirements of machining accuracy and quality for those applications, face gears are mainly manufactured by worm grinding method, of which a dressing wheel is applied to generate the worm surface as its enveloped surface. Based on this manufacturing process, the profile of the dressing wheel should be well defined to make sure the final meshing performance of the face gear drives. In this work, we firstly investigate the mathematical model of dressing wheel with a general profile modification. The worm surface is the envelope to the family of dressing wheel surfaces. Specially, the result is obtained as a closed-form. Subsequently, the face gear tooth surface is calculated as the envelope surface of the worm surface. With the tooth surface models of both face gear and pinion, the tooth contact analysis (TCA) can be computed. According to this method, different parameters for the profile modification of the dressing wheel are compared to improve the working performances by finding the minimal transmission error without edge contacts. The proposed method is validated with simulations.

Nomenclature

γ_0	Initial installation angle of dressing wheel (Fig. 1)
φ_g	An instantaneous position angle of the dressing wheel relative to the worm (Fig. 1)
φ_w	Angle of rotation of the worm (Figs. 1 and 6)
E_g	Shortest distance between two axes of the dressing wheel and the shaper (Figs. 1 and 2)
E_{ws}	Shortest distance between two axes of the worm and the shaper (Figs. 1 and 6)
θ	Angle of rotation of the dressing wheel (Fig. 2)
s_0	The tooth width of the standard rack cutter (Fig. 3)
l_d	The length of $o_r o_0$ (Fig. 3)
α_0	Pressure angle of the standard rack cutter (Fig. 3)
f_d	The offset distance between p_0 and o_0 (Fig. 3)
u_r	Rack cutter profile parameters (Fig. 3)
a_r	Parabolic coefficient of the rack cutter profile (Fig. 3)
p_0	The vertex of the parabola (Fig. 3)
p_r	One point on the rack cutter profile (Fig. 3)
$\mathbf{N}_g$	Normal vector of a point on the surface of the dressing wheel (Fig. 4)
$\mathbf{T}_g$	Tangent vector of a point on the surface of the dressing wheel (Fig. 4)
$\mathbf{T}_{gx}$	The component of $\mathbf{t}_g$ along the direction of x_g (Fig. 4)
$\mathbf{T}_{gz}$	The component of $\mathbf{t}_g$ along the direction of z_g (Fig. 4)
α	The angle between $\mathbf{t}_{gx}$ and $\mathbf{t}_{gz}$ (Fig. 4)
p	One point on the dressing wheel (Fig. 4)
p_h	The intersection of $\mathbf{n}_g$ and z_g (Fig. 4)
h	The distance between the points o_g and p_h (Fig. 4)
ρ	The distance between the points p and p_h (Fig. 4)
φ_s	Angle of rotation of the shaper (Fig. 6)
φ_2	Angle of rotation of the face gear (Fig. 6)
E_{2s}	The distance between the central points of face gear and shaper (Fig. 6)
λ_w	Crossing angle between axes of shaper and worm (Fig. 6)

✉ Yuansheng Zhou
zyszby@hotmail.com

[1] College of Mechanical and Electrical Engineering, Central South University, 410083 Changsha, China

[2] State Key Laboratory of High Performance Complex Manufacturing, Central South University, 410083 Changsha, Hunan, China

1 Introduction

Face gear transmission have many advantages, such as compact structure, convenient installation, large ranges of transmission ratio, and they have been applied in different mech-

anisms in industry. A notable example is that they have been successfully applied in aerospace powertrain system [1, 2]. The other examples are also shown in automobile, fishing tools, electrical devices, etc.

Currently, the manufacturing of face gears is one of the key points to promote their applications in industry. Many researchers took great efforts to study the manufacturing of face gears. Firstly, Litvin et al. [3] used a disc-shaped wheel with an involute profile to develop face gears. Later, to improve the machining accuracy and efficiency, Litvin's group [4–7] proposed the worm grinding method under a special grinding machine developed in Canada North Star Company. The precision of the face gears machined by that equipment can reach the level of AGMA 12. Meanwhile, Zhou et al. [8] proposed a multistep method to completely grind the whole tooth surface of face gear for some special cases. Moreover, the other manufacturing methods were also investigated, such as the plunge milling [9], planing method [10], CNC milling method [11].

Although the worm grinding method can achieve a high machining accuracy and efficiency, it is very difficult to implement this technology due to its complicated process. Especially, it is very challenge to make sure the final working performance is acceptable based on the manufacturing process. In this paper, a new worm grinding method is proposed to the manufacturing of face gears by choosing optimal profile modification parameters of dressing wheel. In Sect. 2, a closed-form representation is proposed to calculate the worm surface, which is the envelope to the family of dressing wheel surface. Subsequently, the face gear tooth surface is calculated as the envelope surface of worm surface in Sect. 3. According to the calculated face gear tooth surface, the TCA is implemented in Sect. 4, and different modification parameters are applied as the optimization variables to find the optimal solution. The proposed method is validated with the simulation in Sect. 5. The conclusion is given in Sect. 6.

2 Calculation of worm surface

2.1 Worm generation process

Face gear is used to transfer power by meshing with a pinion, which can be a cylindrical gear, bevel gear, etc. According to the meshing process, the face gear tooth surface is generated as the envelope to the family of pinion surfaces. In order to avoid the interference during meshing process, the pinion is replaced with a shaper, which has the same tooth geometry as the pinion's but with bigger tooth number. The detail about this idea has been well applied in the design and manufacturing process of face gears [1].

Face gears can be accurately manufactured by the worm grinding with good quality [1, 12]. A schematic diagram is shown in Fig. 1 to illustrate the worm generation process. A dressing wheel is applied to manufacture the worm by simulating the motion of a single shaper tooth moving relative to the worm, whose tooth surface is usually designed as the envelope of a shaper tooth surface [1]. When the worm is machined with the dressing wheel, the relative motion is composed of two motions, the worm rotation along its own axis z_w and the dressing wheel rotation along axis z_s. The ratio of those two rotations is determined according to the transmission ratio of face gear drives [1]. As shown in Fig. 1, φ_w and φ_g are the rotation angles of the worm and dressing wheel, respectively; γ_0 is the initial installation angle of the dressing wheel. E_{ws} is the distance between two axes of x_s and z_w. E_g is the distance between the two central points o_g and o_s. As shown in Fig. 1, the coordinate systems attached to the dressing wheel, worm and shaper are

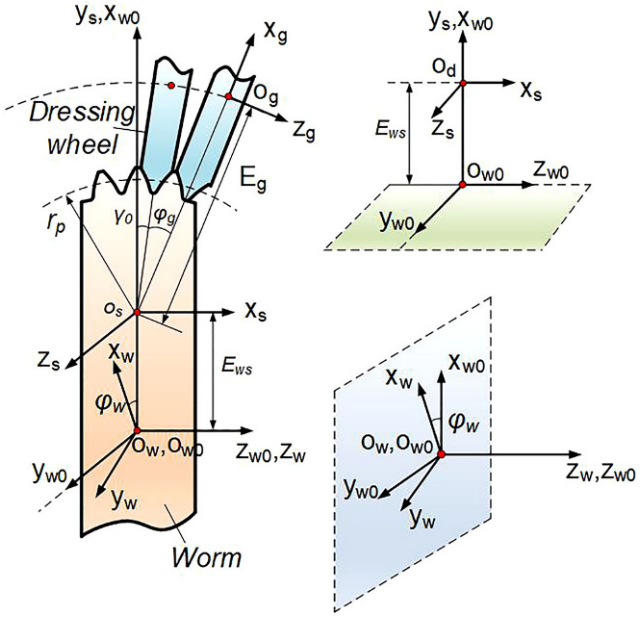

Fig. 1 Worm generation process

assigned as S_g, S_w and S_S, respectively. The transformation matrix from S_g to S_w can be expressed as

$$\mathbf{M}_{wg} = \mathbf{M}_{ww0} \cdot \mathbf{M}_{w0s} \cdot \mathbf{M}_{sg} = \begin{bmatrix} \cos(\varphi_w) & \sin(\varphi_w) & 0 & 0 \\ -\sin(\varphi_w) & \cos(\varphi_w) & 0 & 0 \\ 0 & 0 & 1 & 0 \\ 0 & 0 & 0 & 1 \end{bmatrix} \cdot \begin{bmatrix} 0 & 1 & 0 & E_{ws} \\ 0 & 0 & 1 & 0 \\ 1 & 0 & 0 & 0 \\ 0 & 0 & 0 & 1 \end{bmatrix} \cdot \begin{bmatrix} \sin(\gamma_0+\varphi_g) & 0 & \cos(\gamma_0+\varphi_g) & E_g \cdot \sin(\gamma_0+\varphi_g) \\ \cos(\gamma_0+\varphi_g) & 0 & -\sin(\gamma_0+\varphi_g) & E_g \cdot \cos(\gamma_0+\varphi_g) \\ 0 & 1 & 0 & 0 \\ 0 & 0 & 0 & 1 \end{bmatrix} \tag{1}$$

According to the worm generation process, the worm surface is generated as the envelope surface of the dressing wheel surface moving relative to the worm. In the next subsection, we first introduce the representation of dressing wheel surface, and then calculate the worm surface.

2.2 The representation of dressing wheel surface

As shown in Fig. 2, the surface of dressing wheel is a rotary surface generating by rotating its profile along its own axis z_g. Here, the profile is defined as the same as the profile of a shaper (or a pinion), which is also used to design the tooth surface of face gear [1].

For a general case, the shaper profile is usually modified from a standard involute curve and defined according to its generation process from a rack cutter, as depicted in Fig. 3. a_r is the parabolic coefficient of the rack cutter profile; α_0 is pressure angle; p_0 is the vertex of the parabola, and its position is determined by l_d and f_d; l_d is the distance of $o_r o_0$, and it can be calculated as $l_d = 0.5 s_0 \cdot \cos\alpha_0$, where s_0 represents the space or the tooth width of the standard rack cutter; f_d is the offset distance given as a design parameter.

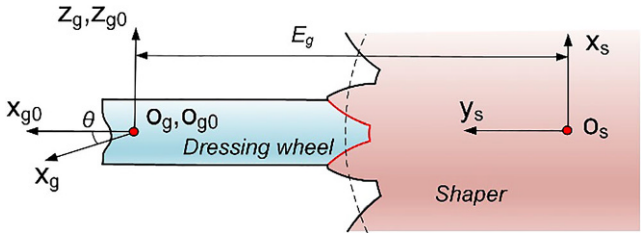

Fig. 2 Tooth profile of dressing wheel

The shaper surface is expressed in the shaper coordinate system S_s as [13, 14].

$$\begin{bmatrix} \mathbf{r}_s(u_r, \theta_r) \\ 1 \end{bmatrix} = \begin{bmatrix} x_r \cdot \cos(\varphi) + y_r \cdot \sin(\varphi) + r_p \cdot \sin(\varphi) - \varphi \cdot r_p \cdot \cos(\varphi) \\ -x_r \cdot \sin(\varphi) + y_r \cdot \cos(\varphi) + r_p \cdot \cos(\varphi) + \varphi \cdot r_p \cdot \sin(\varphi) \\ \theta_r \\ 1 \end{bmatrix} \tag{2}$$

$$\begin{bmatrix} x_r \\ y_r \end{bmatrix} = \begin{bmatrix} \pm(u_r - f_d) \cdot \sin\alpha_0 \mp (l_d + a_r \cdot u_r^2) \cdot \cos\alpha_0 \\ (u_r - f_d) \cdot \cos\alpha_0 + (l_d + a_r \cdot u_r^2) \cdot \sin\alpha_0 \end{bmatrix},$$
$$\varphi = \frac{u_r - f_d + 2a_r \cdot u_r \cdot (l_d + a_r \cdot u_r^2)}{r_p \cdot (\pm\sin\alpha_0 \mp 2a_r \cdot u_r \cdot \cos\alpha_0)} \tag{3}$$

where r_p is the pitch circle radius of the shaper; the upper and lower signs correspond to the left and right sides of rack cutter profile, respectively; θ_r is the coordinate along the axis z_s; φ is the rotation parameter of rack cutter; u_r is the profile parameter of rack cutter; f_d and a_r are two modification coefficients. According to Eq. 2, the shaper surface has the same profile at different sections perpendicular to its axis. Since the dressing wheel profile is the same as the shaper profile, taking the profile in $x_g z_g$ plane as the example, we can obtain it in the dressing wheel coordinate system S_g as

$$\begin{bmatrix} \mathbf{r}_g(u_r) & 1 \end{bmatrix}^{\mathbf{T}} = \mathbf{M}_{gs} \cdot \begin{bmatrix} \mathbf{r}_{sx}(u_r) & \mathbf{r}_{sy}(u_r) & 0 & 1 \end{bmatrix}^{\mathbf{T}} \tag{4}$$

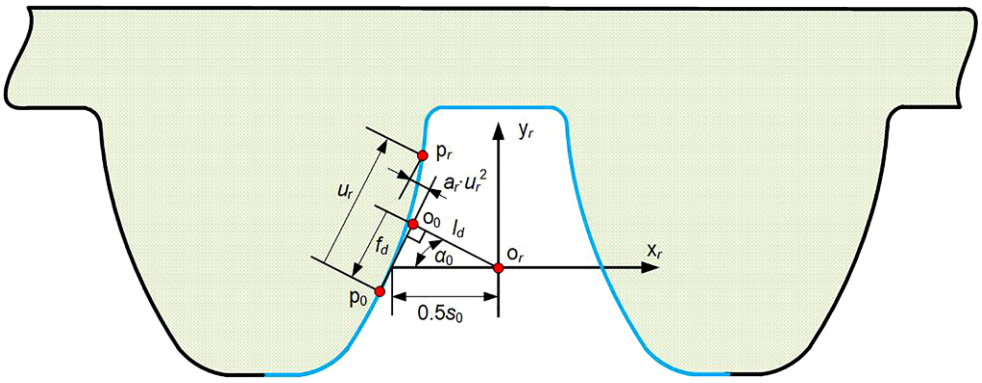

Fig. 3 The profile of a parabolic rack cutter design [13, 14]

According to Eq. 4 (or Eq. 2), the tangent vector of the shaper profile can be derived from its first derivative, and we write it as $\mathbf{t}_s(u_r)$, then the tangent vector of the dressing wheel profile can be obtained as $\mathbf{t}_g(u_r)$.

2.3 A new closed-form vector representation of worm surface

As mentioned in subsection 2.1, the worm surface is generated as the envelope surface of the dressing wheel. Since the dressing wheel is a rotary surface as mentioned in subsection 2.2, its envelope surface can be obtained as a closed-form result according to the geometric meshing theory [15], of which the geometric parameters are shown in Fig. 4.

Based on the worm generation process, the worm surface can be obtained according the geometric meshing theory as [15]

$$\mathbf{r}(u_r,\varphi_g) = \mathbf{o}_g(\varphi_g) + h\cdot\mathbf{l}(\varphi_g) + \rho(u_r)\cdot\mathbf{n}(u_r,\varphi_g) \tag{5}$$

$$\mathbf{n} = \frac{\cos\alpha\cdot\mathbf{v}_h^2}{(\mathbf{l}\times\mathbf{v}_h)^2}\cdot\mathbf{l} - \frac{(\mathbf{l}\cdot\mathbf{v}_h)\cdot\cos\alpha}{(\mathbf{l}\times\mathbf{v}_h)^2}\cdot\mathbf{v}_h \pm \frac{\sqrt{(\mathbf{l}\times\mathbf{v}_h)^2-\cos^2\alpha\cdot\mathbf{v}_h^2}}{(\mathbf{l}\times\mathbf{v}_h)^2}\cdot(\mathbf{l}\times\mathbf{v}_h) \tag{6}$$

Where the angle between normal vector of meshing point and tool axis vector can be expressed as

$$\alpha = \arccos\left(\left|\mathbf{t}_{gx}(u_r)\right| / \left|\mathbf{t}_g(u_r)\right|\right) \tag{7}$$

The distance between the meshing point p and p_h can be expressed as

$$\rho = \mathbf{r}_{gx}(u_r)/\sin\alpha \tag{8}$$

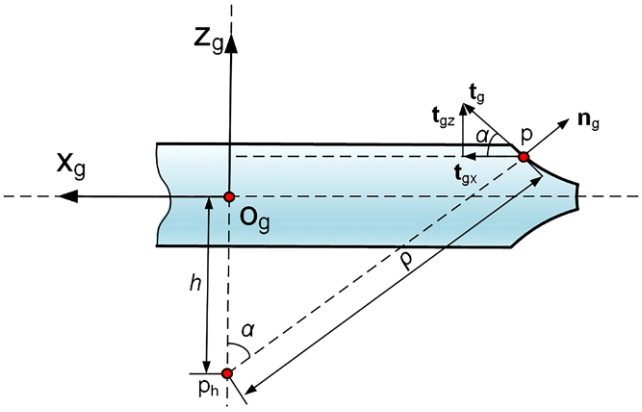

Fig. 4 A generic model to represent the surface of revolution of the generating surface

The distance between the point p_h to the central point $\mathbf{o_g}$ can be expressed as

$$h = \mathbf{r}_{gx}(u_r)\cdot\cot\alpha - \mathbf{r}_{gz}(u_r) \tag{9}$$

The central point of dressing wheel at any time can be expressed as

$$\begin{bmatrix}\mathbf{o_g}\\1\end{bmatrix} = \mathbf{M}_{wg}\cdot\begin{bmatrix}0\\0\\0\\1\end{bmatrix} = \begin{bmatrix}\cos(\varphi_w)\cdot(E_{ws}+E_g\cdot\cos(\gamma_0+\varphi_g))\\-\sin(\varphi_w)\cdot(E_{ws}+E_g\cdot\cos(\gamma_0+\varphi_g))\\E_g\cdot\sin(\gamma_0+\varphi_g)\\1\end{bmatrix} \tag{10}$$

The unit cutter axis vector of the dressing wheel at any time can be expressed as

$$\mathbf{l} = \left[-\sin(\gamma_0+\varphi_g)\cdot\cos(\varphi_w) \quad \sin(\gamma_0+\varphi_g)\cdot\sin(\varphi_w) \quad \cos(\gamma_0+\varphi_g) \quad 0\right]^{\mathbf{T}} \tag{11}$$

The velocity $\mathbf{v_h}$ of point p_h during the generating process can be obtained as

$$\mathbf{v_h} = \frac{d\,\mathbf{o_g}(\varphi_g)}{d\,\varphi_g} + h\cdot\frac{d\,\mathbf{l}(\varphi_g)}{d\,\varphi_g} \tag{12}$$

By submitting Eqs. 6–12 into Eq. 5, we can obtain the explicitly expression of tooth equation of the worm surface. The model of worm surface calculated by the explicitly expression shown in Fig. 5.

3 The calculation of face gear tooth surface generated by worm grinding

The generation process of worm grinding face gears are shown in Fig. 6a. φ_w and φ_2 are two rotation angles of worm and face gear, respectively. E_{2s} is the distance from the center point of worm to the center point of shaper. The generation process includes three movements. 1) The Face gear is rotating along its axis with an angular velocity

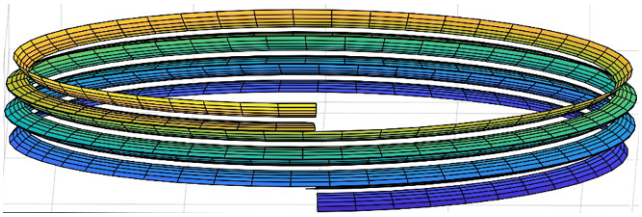

Fig. 5 Model of worm surface

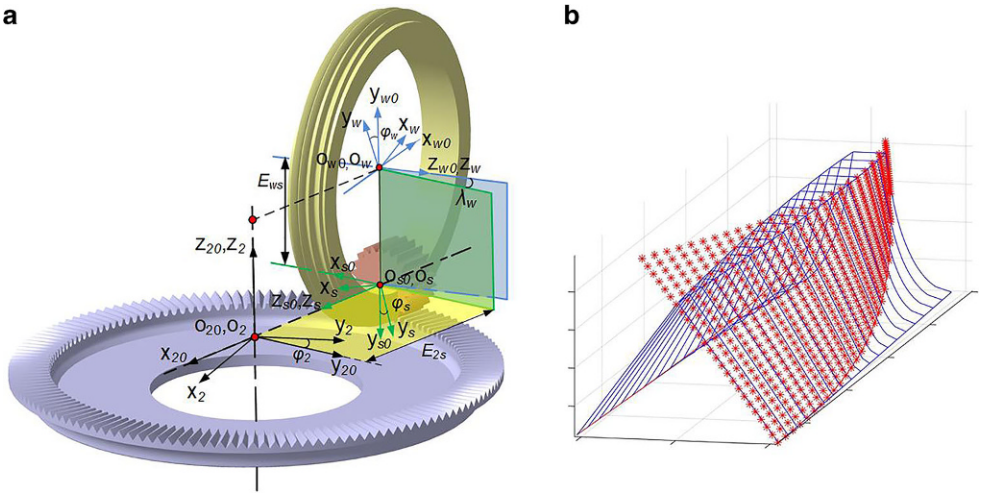

Fig. 6 **a** Schematic diagram of worm enveloping face gear [7]. **b** Face gear tooth surface points obtained by worm enveloping

ω_2. 2) The worm is rotating along its axis with an angular velocity ω_w. 3) The worm is feeding along the radial direction of face gear at a speed v_w. The movements 1) and 2) meet the transmission ratio relationship as $\omega_2/\omega_w = N_w/N_2$. With the above three movements, the worm can grind the complete face gear tooth surface. Subsequently, the tooth equation of the face gear $\mathbf{r}_2$ can be expressed in the face gear attached coordinate system S_2 as

$$\begin{cases} \mathbf{r}_2(u_r,\varphi_g,\varphi_w,E_{2s}) = \mathbf{M}_{2w}(\varphi_w,E_{2s}) \cdot \mathbf{r}_w(u_r,\varphi_g) \\ \mathbf{N}_w(u_r,\varphi_g) \cdot \mathbf{v}_w^{(w2,E_{2s})} = f_{w2}^{(1)}(u_r,\varphi_g,\varphi_w,E_{2s}) = 0 \\ \mathbf{N}_w(u_r,\varphi_g) \cdot \mathbf{v}_w^{(w2,\varphi_w)} = f_{w2}^{(2)}(u_r,\varphi_g,\varphi_w,E_{2s}) = 0 \end{cases} \quad (13)$$

The matrix $\mathbf{M}_{2w}$ is the transformation matrix from the coordinate system S_w to S_2, and the first meshing equation represents the situation that the rotation parameter φ_w is constant while the feed parameter E_{2s} is changed; the second represent the situation that the feed parameter E_{2s} is constant while the rotation parameter φ_w is changed. It can be found from Fig. 6b that the enveloped surface of face gear coincides with the theoretical surface, that proves the correctness of the worm enveloping face gear principle and the new worm surface modeling method.

4 Influence of the modification of dressing wheel parameters on TCA results

In order to improve the meshing performances of the face gear drive, the modification of dressing wheel parameters is applied to study the influence on contact path and transmission error of the face gear drive. The example about the face drives is given with the data shown in Table 1. Based on this example, two kinds of modifications for the position parameter and parabolic parameter, respectively, are implemented as follows.

4.1 Influence of the position parameter modification

For this research, the position parameter modification of face gear f_d is changed, while the parabolic parameter a_r was taken 0.002. The calculation results are shown in Fig. 7. It can be seen that the contact paths are curves that curve from the outside to the inside of the face gear tooth surface and the transmission error curves approximate parabolas. As the parameter f_d increasing, the contact paths gradually shift toward the inner side of the face gear, and the maximum value of the transmission error becomes smaller firstly but then becomes bigger. For the values of f_d we taken, when it equals 0.8 the maximum value of transmission error is smallest about 4.3×10^{-5} /rad.

Table 1 Design parameters of the modified straight tooth face gear transmission system

Modified face gear transmission system parameters	Designed parameters value
Tooth number of shaper N_s	22
Tooth number of pinion N_1	20
Tooth number of face gear N_2	142
Pressure angle α/(°)	25
Modulus m (mm)	1.95
Distance between two axes of the worm and the shaper E_{ws} (mm)	100
Worm lead angle λ_m/(°)	0.46
Position parameter of modification f_d (mm)	Variable
Parabolic parameter of modification a_r	Variable
Parabolic parameter of pinion a_1	0
Inner radius of the face gear R_1/mm	134
Outer radius of the face gear R_2/mm	155

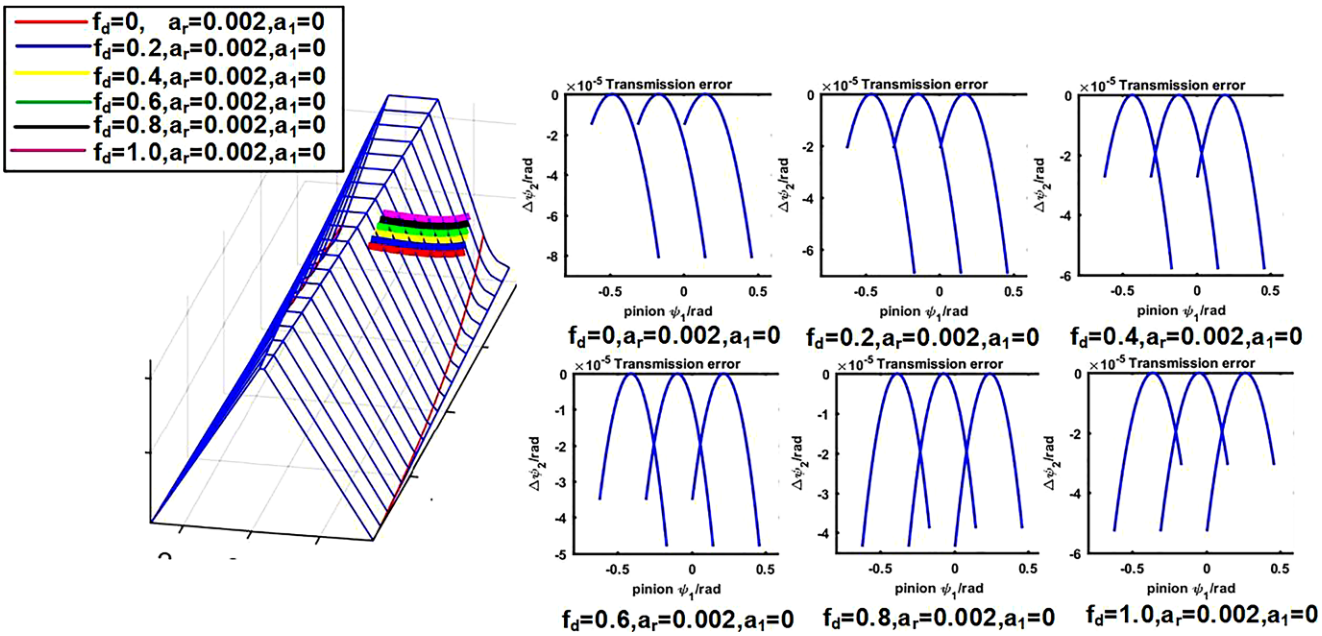

Fig. 7 TCA results of the modification of position parameter

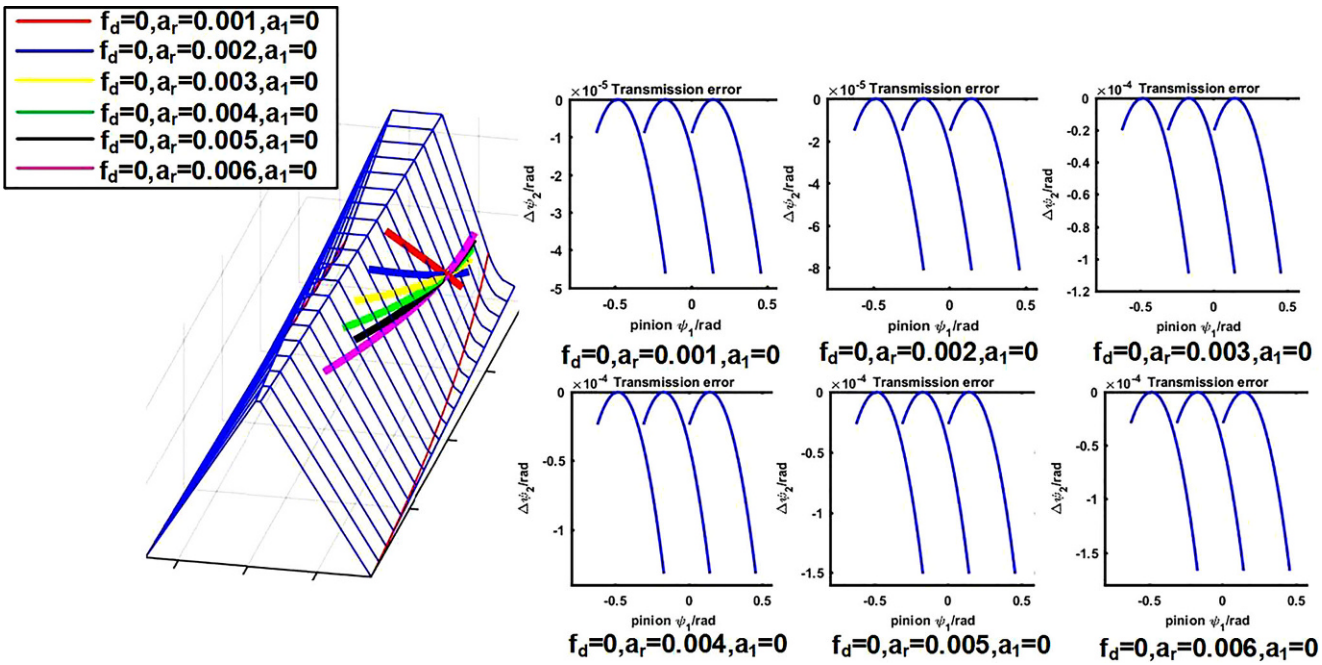

Fig. 8 TCA results of the modification of parabolic parameter

4.2 Influence of the parabolic parameter modification

For this research, the value of the parabolic parameter a_r is changed, while the position value f_d was taken 0, the calculation results are shown in Fig. 8. It can be seen that the contact paths on the face gear become curves that curve from the outside to the inside of the face gear tooth surface and the transmission error curves approximate parabolas. As parameter a_r increasing, the contact paths gradually deflect toward the root of the face gear, the maximum value of the transmission error becomes bigger. For the values of a_r we taken, when it equals 0.01 the maximum value of transmission error is smallest about 4.8×10^{-5}/rad.

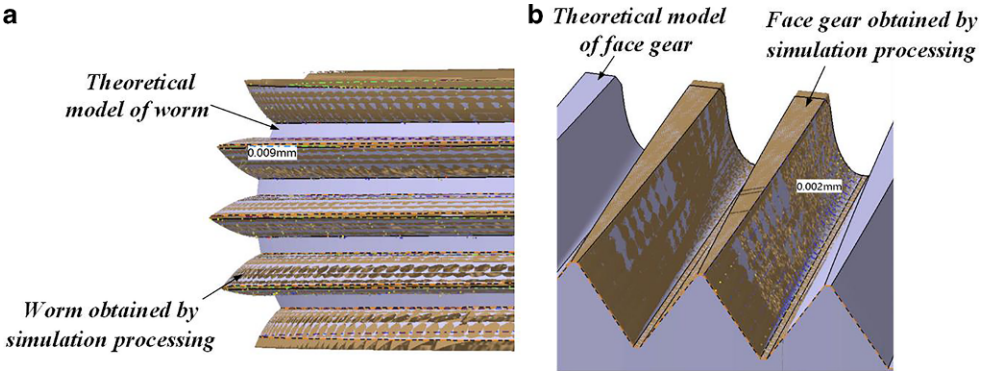

Fig. 9 Comparison of worm and face gear theory and simulation model

5 Simulation verification

In this work, a virtual universal five-axis CNC machine tool was used to conduct the manufacturing simulation of worm surface and face gear, whose basic parameters shown in Table 1, in commercial software VERICUT. Both modified parameters f_d and a_s are given as 0.8 and 0.01, respectively. The result is shown in Fig. 9 that the tooth surface deviations of the worm surface and the face gear are less than 10 μm, and most area are about 2 μm. The results are in line with expectation and verify the correctness of the previous theoretical analysis.

6 Conclusions

A new worm grinding method of face gears is studied, and the worm is machined with a dressing wheel. Several distinguished points of this work are stated as follows.

1) The worm surface is calculated as a new closed-form vector result. As the envelope to the family of worm surfaces, the tooth surface of face gear is calculated with a method of two-parameter envelope.
2) By changing the modification parameters of the dressing wheel, an optimized profile of the dressing wheel is calculated to improve the working performance with the minimal transmission error and acceptable contact path.
3) The grinding process of the face gear in a universal five-axis CNC machine tool is simulated in VERICUT. According to the comparison between the results of simulation and calculation, the proposed method is valid.

References

1. Litvin FL, Fuentes A (2004) Gear Geometry and Applied Theory. Cambridge University Press, Cambridge, ISBN 978-0-5218-1517-8
2. Litvin FL, Wang JC, Bossler RB, Chen YJ, Heath G, Lewicki DG (1994) Application of facegear drives in helicopter transmissions. J Mech Des 116(3):672–676
3. Litvin FL, Egelja A, Tan J, Heath G (1998) Computerized design, generation and simulation of meshing of orthogonal offset face-gear drive with a spur involute pinion with localized bearing contact. Mech Mach Theory 33(1–2:87–102
4. Litvin FL, Hsiao CL (1994) Computerized Simulation of Generation of Internal Involute Gears and Their Assembly, Transactions of ASME. J Mech Des 116:683–689
5. Litvin FL et al (1996) Apparatus and method for precision grinding face gear. US-Patent 6.146.253. https://patentimages.storage.googleapis.com/a1/49/67/72737f55a7bdbe/US6146253.pdf
6. Litvin FL, Wang JC, Bossler RB et al (1994) Application of Face-Gear Drives in Helicopter Transmissions. J Mech Des 116(3):672
7. Litvin FL, Fuentes A, Zanzi C et al (2002) Face-gear drive with spur involute pinion: geometry, generation by a worm, stress analysis. Comput Methods Appl Mech Eng 191((25–26):2785–2813
8. Zhou Y, Tang J, Zhou H, Yin F (2016) Multistep Method for Grinding Face-Gear by Worm. J Manuf Sci Eng 138:71013–71018
9. Yang X, Tang J (2014) Research on manufacturing method of CNC plunge milling for spur face-gear. J Mater Process Tech 214:3013–3019
10. Tang J, Yang X (2016) Research on manufacturing method of planing for spur face-gear with 4-axis CNC planer. Int J Adv Manuf Technol 82:847–858
11. Zhou Y, Wang S, Wang L, Tang J, Chen Z (2019) CNC milling of face gears with a novel geometric analysis. Mech Mach Theory 139:46–65
12. Zhou W, Tang J, Chen H, Shao W, Zhao B (2019) Modeling of tooth surface topography in continuous generating grinding based on measured topography of grinding worm. Mech Mach Theory 131:189–203
13. Wu Y, Zhou Y, Zhou Z et al (2018) An advanced cad/cae integration method for the generative design of face gears. Adv Eng Softw 126:90–99
14. Zhou Y, Wu Y, Wang L, Tang J, Ouyang H (2019) A new closed-form calculation of envelope surface for modeling face gears. Mech Mach Theory 137:211–226
15. Zhou Y, Chen Z (2015) A new geometric meshing theory for a closed-form vector representation of the face-milled generated gear tooth surface and its curvature analysis. Mech Mach Theory 83:91–108